

## H<sub>2</sub> IMAGING OF SANDQVIST 136: SHOCKED GAS, JETS, AND KNOTS<sup>1</sup>

J. L. YUN,<sup>2</sup> DAN P. CLEMENS,<sup>3</sup> M. C. MOREIRA,<sup>2</sup> AND N. C. SANTOS<sup>2</sup>

Received 1996 October 21; accepted 1997 January 24

### ABSTRACT

We present a study of the morphological aspects of H<sub>2</sub> jets and knots seen toward the small dark cloud Sandqvist 136. Near-infrared images of this cloud in the *J*, *H*, and *K* bands and in the 2.12 μm *v* = 1–0 *S*(1) molecular hydrogen line were obtained. The images reveal the presence of a near-infrared nebula with a conical shape. The location of the apex of the cone, in the *K*-band image, coincides with the position of an *IRAS* Point Source Catalogue source. This source, possibly a class 0 young stellar object, is likely to be the illuminator of the nebula. The position and orientation of the conical nebula coincide with those of the blueshifted lobe of the previously found molecular outflow associated with Sandqvist 136. Near-infrared jets and knots were found positionally associated with the high-velocity molecular outflow. The knots seem to be tracing the walls of a cavity excavated by the molecular outflow. Unlike most outflows commonly associated with class 0 sources, the outflow associated with this source appears to be poorly collimated.

*Subject heading:* infrared: stars — ISM: clouds — ISM: globules — ISM: individual (Sandqvist 136) — ISM: jets and outflows — stars: formation — stars: mass loss

### 1. INTRODUCTION

Mass ejection from young stars constitutes one of the major signposts of star formation in a molecular cloud. The ejection of mass may be detected in the form of more or less collimated high-velocity winds, jets, and molecular outflows (e.g., Mundt 1993) occurring simultaneously with the accretion of material from the surroundings of the star. The flow of gas ejected from the vicinity of the forming star results in the entrainment of ambient gas that may develop shocks, seen as nebular emission rich in spectral lines, both in optical and in near-infrared wavelengths.

Sandqvist 136 (Sandqvist & Lindroos 1976; Sandqvist 1977), also designated DC 297.7–2.8 (Hartley et al. 1986) and BHR 71 (Bourke, Hyland, & Robinson 1995), is a small dark cloud in the southern sky, relatively isolated, and with a regular shape (see Fig. 1 obtained from the Digital Sky Survey<sup>4</sup>). It is located near the Coalsack dark cloud at a distance of 200 pc (Seidensticker & Schmidt-Kaler 1989) and belongs to the class of clouds named small Bok globules (Bok & Reilly 1947), the smallest and simplest molecular structures in the interstellar medium capable of forming stars (e.g., Yun & Clemens 1990, 1994).

Star formation activity in Sandqvist 136 was first identified in broadband *J*-, *H*-, and *K*-band imaging, by Bourke et al. (1993), which revealed the presence of an optically invisible object roughly coincident with an *IRAS* point source (IRAS 11590–6452). In addition, this young stellar object drives a high-velocity molecular outflow (Garay, Köhnenkamp, &

Rodriguez 1996; Bourke et al. 1997) oriented north (redshifted lobe)–south (blueshifted lobe). Interestingly, Garay et al. (1996), using multimolecular observations toward this cloud, found a strong enhancement in the abundance of silicon monoxide and methanol in the lobes of the outflow, with line profiles indicating that shocks are the mechanisms responsible for the excitation of these species.

Shock structures at low and intermediate velocities (up to 30–50 km s<sup>−1</sup>) have been found to be well traced by molecular hydrogen emission at 2.121 μm (e.g., Smith 1993; Davis, Mundt, & Eisloffel 1994c; McCaughrean, Rayner, & Zinnecker 1994). In this study of Sandqvist 136, we have searched for the presence of shock-excited material positionally associated with the molecular outflow. We found a wealth of shock-related phenomena (near-infrared jets and knots) that are likely to be associated with the previously discovered molecular outflow. In the next sections, we describe our observations, and present and discuss the results.

### 2. OBSERVATIONS AND DATA REDUCTION

Near-infrared imaging observations toward Sandqvist 136 were carried out during the night of 1996 May 6 using the IRAC2 NICMOS 3 infrared array camera (Moorwood et al. 1992) mounted on the ESO 2.2 m telescope, at La Silla, Chile. We obtained images in the *J*, *H*, and *K* bands (at 1.25, 1.65, and 2.2 μm, respectively) and in the 2.12 μm *v* = 1–0 *S*(1) molecular hydrogen line (FWHM = 0.039 μm). The NICMOS 3 array contains 256 × 256 pixels and was used at a plate scale of 0".52 pixel<sup>−1</sup>, resulting in a field of view of 2.2 × 2.2 arcmin<sup>2</sup> on the sky. We obtained a set of nine dithered frames in the *J*, *H*, and *K* bands and 4 × 6 dithered frames in the H<sub>2</sub> line. The dithering offsets were 1', both in right ascension and in declination, in the *J*, *H*, and *K* bands, and 40" and 1', respectively, in right ascension and in declination, in H<sub>2</sub>. The total integration time per frame was 20 s in the *H* and *K* bands, 30 s in *J*, and 150 s in H<sub>2</sub>. The night was not truly photometric, and we thus restrict our study to an analysis of the morphological aspects of the features seen in the images.

Reduction of the images was performed by subtraction of a

<sup>1</sup> Based on observations at the European Southern Observatory, La Silla, Chile.

<sup>2</sup> Departamento de Física, Universidade de Lisboa, Campo Grande, Edif. C1, 1700 Lisboa, Portugal; yun@delphi.cc.fc.ul.pt, miguelm@delphi.cc.fc.ul.pt, nuno@astro.cc.fc.ul.pt.

<sup>3</sup> Department of Astronomy, Boston University, 725 Commonwealth Avenue, Boston, MA 02215; clemens@protostar.bu.edu.

<sup>4</sup> Based on photographic data obtained using the UK Schmidt Telescope. The UK Schmidt Telescope was operated by the Royal Observatory Edinburgh, with funding from the UK Science and Engineering Research Council, until 1988 June, and thereafter by the Anglo-Australian Observatory. The Digitized Sky Survey was produced at the Space Telescope Science Institute under US Government grant NAG W-2166.

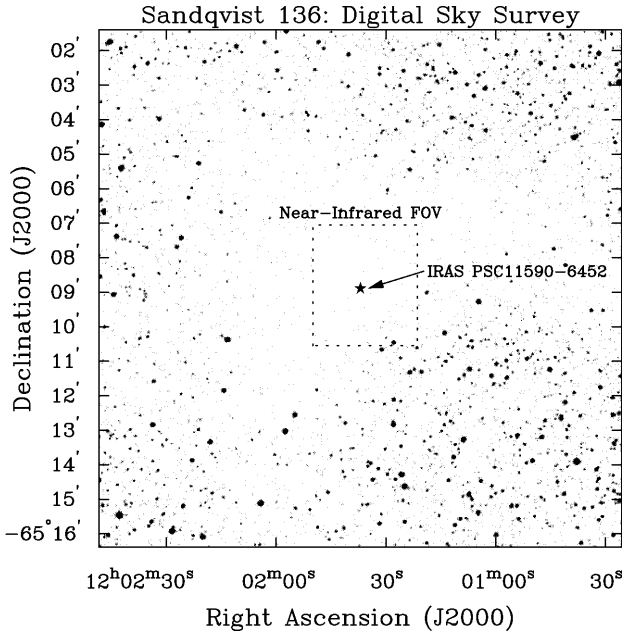


FIG. 1.—Optical image of Sandqvist 136 (from the Digital Sky Survey) covering  $15' \times 15'$ . The cloud has a general shape of a “croissant” with a high-opacity core and a concave edge facing southwest. The approximate size and location of the near-infrared imaging field of view are shown by the dotted box.

sky frame (computed by median-filtering of the dithered images) followed by flat-fielding. The final flat-fielded images were subsequently corrected for the presence of bad pixels and mosaicked, co-adding the overlapping regions.

### 3. RESULTS AND DISCUSSION

Figure 2 presents the resulting images centered at the position of IRAS 11590–6452 ( $\alpha_{1950} = 11^{\text{h}}59^{\text{m}}03^{\text{s}}$ ,  $\delta_{1950} = -64^{\circ}52'11''$ ). The figures cover an area of about  $3'.0 \times 3'.5$ . An immediate and outstanding feature in these images is the presence of the conical-shaped object at the center of the images. However, before turning our attention to this remarkable object, we will address the morphology and opacity of the cloud.

#### 3.1. Morphology and Opacity of Sandqvist 136

The Digital Sky Survey plates (Fig. 1) reveal the general shape of the cloud. Like Bok globule CB 34 (Alves & Yun 1995; Moreira & Yun 1995), Sandqvist 136 has the general shape of a “croissant,” with a high-opacity central region and a concave edge facing southwest where several field stars can be seen in Figure 2 (*upper left panel*). In addition, the *J*-, *H*-, and *K*-band images reveal that within the cloud core, the northern region is quite opaque, since several background (or embedded) stars can be seen in the *K*-band image but are absent in the *J*-band image. Even though the night was not photometric (which prevents obtaining absolute photometry), it is possible to do relative photometry. A comparison of relative near-infrared colors of several stars contained in the *H*- and *K*-band images reveals that, on average, extinction decreases gradually from the northeastern corner toward the southwest.

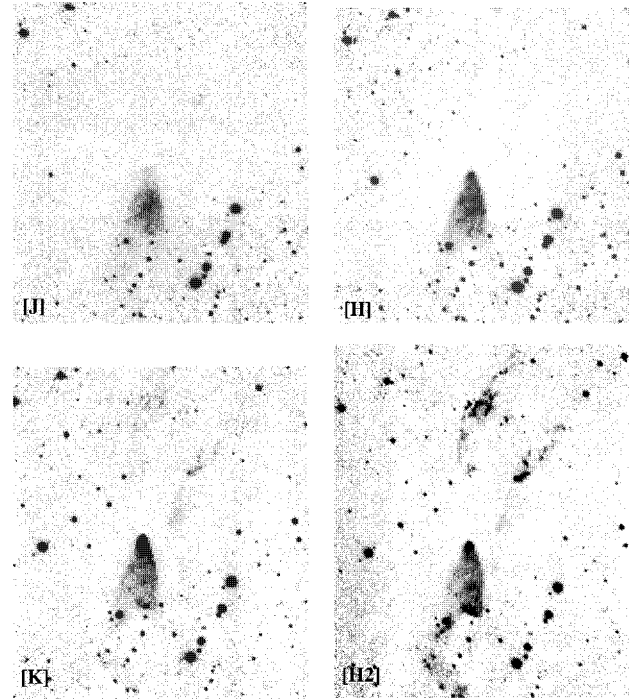


FIG. 2.—Near-infrared images of Sandqvist 136 covering about  $3'.0 \times 3'.5$ . North is up, and east to the left: (*upper left panel*) *J* band; (*upper right panel*) *H* band; (*lower left panel*) *K* band; (*lower right panel*)  $\text{H}_2$ . Notice, near the center, the presence of a near-infrared conical nebula. IRAS 11590–6452 is located at the position of the apex of the nebula. The gray-scale levels were chosen such that continuum sources appear approximately equally bright in the *K*-band and  $\text{H}_2$  images. Notice also the presence of multiple knots and apparent diffuse emission in the  $\text{H}_2$  image.

#### 3.2. The Central Object

An outstanding near-infrared object lies at the center of our images. It appears as a stellar-like source surrounded by a near-infrared nebula of conical shape extending toward the south. The *IRAS* source PSC 11590–6452 (hereafter called IRS) is located at the position of the apex of the nebula.

The position and orientation of the conical nebula coincide with those of the blueshifted lobe of the molecular outflow associated with Sandqvist 136 (Garay et al. 1996; Bourke et al. 1997). Moreover, a comparison of the *K*-band (Fig. 2, *lower left panel*) and the *J*-band (Fig. 2, *upper left panel*) images indicates that the fan-shaped nebulosity is bluer than the compact peak (which seems to be the stellar object) at the apex of the fan. Taken together, these facts imply that the conical nebulosity is due to light from the object scattering off the walls of a cavity excavated by the high-velocity outflow.

Further analysis of the near-infrared images reveals that the central stellar-like object has a much broader profile than that of the field stars. In addition, relative to another star in the frame, there is a progression in the positions of the “stellar-like” object in the *J*-, *H*-, and *K*-band images. The progression is almost exactly in a north-south direction, with the position in the *K* band located  $1''$  north of the position in the *H* band, which is itself located about  $1'.5$  north of the position in the *J* band. This behavior is typical of what is predicted for the appearance of an object seen due to scattering of light. As a result, we conclude that we may not be seeing the near-infrared counterpart to the *IRAS* source PSC 11590–6452.

Models of embedded infrared nebulae have been computed

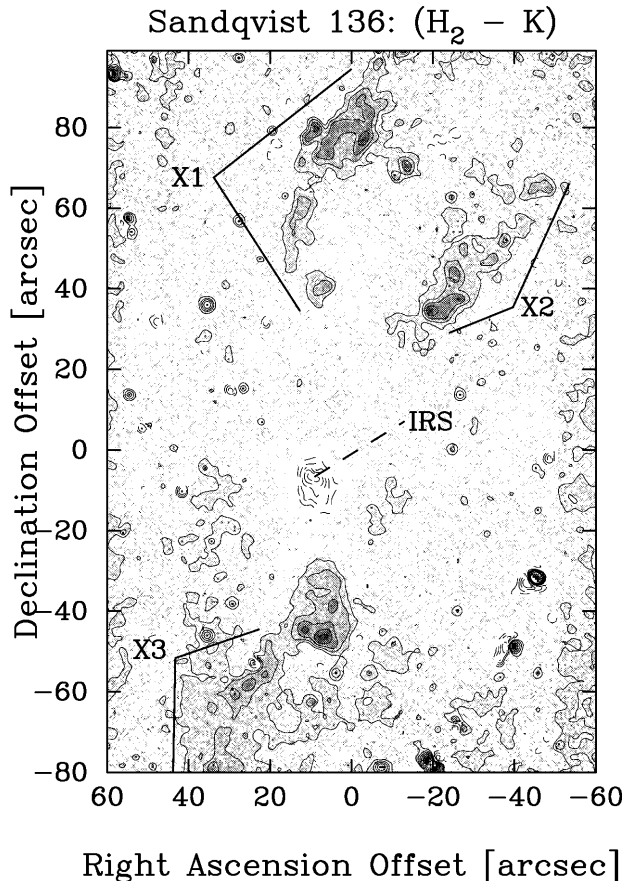


FIG. 3.—Continuum-subtracted H<sub>2</sub> image (H<sub>2</sub> - K) with superimposed isophotes. The image was convolved with a 0".7 FWHM gaussian before being contoured. The axes give the coordinates relative to IRAS 11590-6452.

by Lazareff, Pudritz, & Morin (1990), Whitney & Hartmann (1992), (1993), and Kenyon et al. (1993). The shapes of the infrared nebulae predicted by the models of Whitney & Hartmann (1993) include conical shapes that are similar to the appearance of this nebula. In particular, the nebula is well matched by two of the Whitney & Hartmann (1993) models (Nos. 5 and 6, with projection cosines  $\mu = 0.6$ ;  $\mu = 0$  corresponding to edge-on). A moderately to highly inclined bipolar cavity excavated by gas from a wind from the central source is thus inferred, with the redshifted lobe that carries the flow farther into the cloud being suppressed below our detection threshold by the large optical depths associated with the dust envelope surrounding the cavity.

### 3.3. Shocks, Jets, and Knots

In the lower panels of Figure 2, we present, respectively, the K-band and H<sub>2</sub> near-infrared images of Sandqvist 136. The gray-scale levels were chosen such that continuum sources appear approximately equally bright in both images. Notice, in the central top half of the images, the presence of several features in the H<sub>2</sub> image that are much fainter in the K-band image. Similar features are also seen in the central lower half of the H<sub>2</sub> image, including some knots seen through the conical nebula. The features that are absent or barely present in the K-band image represent shocked molecular hydrogen emission.

In Figure 3, we present the continuum-subtracted H<sub>2</sub> image

(H<sub>2</sub> - K) with superimposed isophotes. In this image, the features seen are almost entirely due to line emission from shocked molecular hydrogen. The irregular contours appearing on both sides of the image are due to the higher background noise in the regions of the mosaic where fewer frames were co-added.

Interestingly, the conical nebula is smaller and more offset from IRS in this difference image compared with the H<sub>2</sub> or the K-band images. This seems to indicate that the region of brightest reflections is closer to IRS and the regions of shocked H<sub>2</sub> are farther from IRS. Alternatively, the absence of emission near IRS in the difference image could be due to the larger extinction closer to IRS than farther south.

In Figure 3, we identify three groups of knots, designated by X1, X2, and X3. The X1 structure looks very similar to the L1448 H<sub>2</sub> curving jet (Davis et al. 1994a), where the curvature of the jet is explained by a string of shocks produced by the stellar wind as it encounters increasing ambient gas densities and the flow is refracted (note how X1 curves away from the more opaque northeastern region). In applying this scenario to Sandqvist 136, the X1 H<sub>2</sub> knots would be tracing the curving jet and would correspond to oblique shocks associated with the interface between the stellar wind from the central source and the surrounding molecular gas.

On the other hand, the locations of the X1 and X2 groups of knots follow the redshifted CO lobe of Garay et al. (1996) and Bourke et al. (1997). If we connect up the knots along X1 and along X2, they seem to arc back to the IRS source. These two arcs, with a maximum separation of about 1', may be tracing out the tangential walls of the red lobe, where molecular gas entrainment is likely to occur and conditions for H<sub>2</sub> line formation prevail. Similarly, although fainter, more diffuse, and difficult to follow (thus more uncertain), the X3 knots are located along portions of the blue CO lobe, allowing the same interpretation. The "opening angles" to X1-X2 and to X3 are about 35°-40°, and fairly symmetric to the north and south with respect to the position of IRS. Our observations support the idea that H<sub>2</sub> emission arises in the boundary between the outflow and the ambient gas, such as in the cases of HH 46/47 and HH 1 (Eisloffel et al. 1994; Davis et al. 1994b), where the H<sub>2</sub> emission outlines what appears to be an evacuated cavity.

Seeing optical manifestations of the stellar wind (bow shocks, HH objects) from IRS is precluded by the high extinction produced by the cloud. Therefore, we cannot use the spatial relationship between optical and infrared lines to distinguish between different scenarios of excitation of the molecular emission. However, the near-infrared data available give some indication about the type of molecular gas entrainment taking place in Sandqvist 136. The transfer of momentum from a jet to the ambient molecular gas may happen by prompt entrainment or by steady entrainment (De Young 1986). In prompt entrainment, the bow shock at the head of a jet pushes the molecular material ahead and to the sides of the bow. Steady entrainment occurs along the sides of the jet when the ambient gas is dragged by the jet. A comparison of the H<sub>2</sub> knots seen in our images with modeling of H<sub>2</sub> emission by Hartigan et al. (1996) seems to indicate that prompt entrainment with multiple bow shocks is occurring. As with other objects (e.g., HH 46/47), the presence of clumpy molecular shells is consistent with prompt entrainment but less so with steady entrainment.

3.4. *A Class 0 or a Class I Source?*

IRAS 11590–6452 is optically invisible, most likely not seen in the near-infrared *J* or *H* bands, and is likely to be invisible in the *K* band also. However, it displays an extended near-infrared nebula, and its *IRAS* fluxes, from 12 to 100  $\mu\text{m}$ , rise steeply toward the longer wavelengths, suggesting that this source could be classified as an extreme class I source (Adams, Lada, & Shu 1987). However, Bourke et al. (1997) measured the 1.3 mm flux (1.7 Jy) and determined the bolometric luminosity of IRAS 11590–6452 to be  $9 L_{\odot}$ . They find that  $L_{\text{submm}}/L_{\text{bol}} \sim 2 \times 10^{-2}$ , which satisfies the class 0 criterion ( $L_{\text{submm}}/L_{\text{bol}} > 5 \times 10^{-3}$ ) of André, Ward-Thompson, & Barsony (1993) for sources whose circumstellar masses are larger than the masses of the central objects. Similarly, the 1.3 mm flux places this source in the region of class 0 sources of the Saraceno et al. (1996) ( $L_{\text{bol}}$ ,  $S_{1.3\text{mm}}^{160\text{pc}}$ ) diagram (Ward-Thompson et al. 1995; Saraceno et al. 1996). Hence, IRAS 11590–6452 may be classified either as a class 0 source displaying a near-infrared reflection nebula or as an extreme class I source. It is one more example of a very young stellar source that exhibits a near-infrared nebula, because of either an inclination effect (protostellar envelopes are not strictly spherical) or a more extended, less dense protostellar cocoon, associated with the presence of an excavated cavity. Other similar examples are K4166 in Taurus (Bontemps et al. 1996) and CB 54 (Yun 1996).

## 4. CONCLUSIONS

Sandqvist 136 (BHR 71), a nearby southern small dark cloud, displays many signs of being the host for active star formation phenomena. Near-infrared images reveal the presence of a conical reflection nebula. The location of the apex of the cone, in the *K*-band image, coincides with the position of IRAS 11590–6452. This source, possibly a class 0 young stellar object, is likely to be the illuminator of the nebula, but it may have avoided detection in the near-infrared images.

The conical nebula is due to light from the central source scattering off the walls of an inclined bipolar cavity.  $\text{H}_2$  bright knots in the lobes of the molecular outflow are likely tracing shocked hydrogen emission seen through the tangents of the lobe cavity walls, where gas entrainment should occur. Unlike most outflows commonly associated with class 0 sources, the outflow associated with this source appears poorly collimated.

We thank T. Bourke for helpful comments. This work has been partially supported by a JNICT grant to J. L. Y. Support from JNICT to M. C. M. and N. C. S. in the form of a scholarship is gratefully acknowledged.

## REFERENCES

- Adams, F. C., Lada, C. J., & Shu, F. H. 1987, *ApJ*, 312, 788  
 André, P., Ward-Thompson, D., & Barsony, M. 1993, *ApJ*, 406, 122  
 Alves, J. F., & Yun, J. L. 1995, *ApJ*, 438, L107  
 Bok, B. J., & Reilly, E. F. 1947, *ApJ*, 105, 255  
 Bontemps, S., André, P., Terebey, S., & Cabrit, S. 1996, *A&A*, 311, 858  
 Bourke, T. L., et al. 1997, *ApJ*, 476, 781  
 Bourke, T. L., Hyland, A. R., & Robinson, G. 1995, *MNRAS*, 276, 1052  
 Bourke, T. L., Hyland, A. R., Robinson, G., & James, S. D. 1993, *Proc. Astron. Soc. Australia*, 10, 236  
 Davis, C. J., Dent, W. R. F., Matthews, H. E., Aspin, C., & Lightfoot, J. F. 1994a, *MNRAS*, 266, 933  
 Davis, C. J., Eisloffel, J., & Ray, T. P. 1994b, *ApJ*, 426, L93  
 Davis, C. J., Mundt, R., & Eisloffel, J. 1994c, *ApJ*, 437, L55  
 De Young, D. 1986, *ApJ*, 307, 62  
 Eisloffel, J., Davis, C. J., Ray, T. P., & Mundt, R. 1994, *ApJ*, 422, L91  
 Garay, G., Köhnenkamp, I., & Rodriguez, L. F. 1996, *Messenger*, 83, 31  
 Hartigan, P., Carpenter, J. M., Dougados, C., & Skrutskie, M. F. 1996, *AJ*, 111, 1278  
 Hartley, M., Manchester, R. N., Smith, R. M., Triton, S. B., & Goss, W. M. 1986, *A&AS*, 63, 27  
 Kenyon, S. J., Whitney, B. A., Gomez, M., & Hartmann, L. 1993, *ApJ*, 414, 773  
 Lazareff, B., Pudritz, R. E., & Morin, J. L. 1990, *ApJ*, 358, 170  
 McCaughrean, M. J., Rayner, J. T., & Zinnecker, H. 1994, *ApJ*, 436, L189  
 Moorwood, A., et al. 1992, *Messenger*, 69, 61  
 Moreira, M. C., & Yun, J. L. 1995, *ApJ*, 454, 850  
 Mundt, R. 1993, in *Stellar Jets and Bipolar Outflows*, ed. L. Errico & A. Vittone (Dordrecht: Kluwer), 91  
 Sandqvist, A. 1977, *A&A*, 57, 467  
 Sandqvist, A., & Lindroos, K. P. 1976, *A&A*, 53, 179  
 Saraceno, P., André, P., Ceccarelli, C., Griffin, M., & Molinari, S. 1996, *A&A*, 309, 827  
 Seidensticker, K. J., & Schmidt-Kaler, Th. 1989, *A&A*, 225, 192  
 Smith, M. D. 1993, *ApJ*, 406, 520  
 Ward-Thompson, D., Scott, P. F., Hills, R. E., & André, P. 1995, *Ap&SS*, 224, 47  
 Whitney, B. A., & Hartmann, L. 1992, *ApJ*, 395, 529  
 ———. 1993, *ApJ*, 402, 605  
 Yun, J. L. 1996, *AJ*, 111, 930  
 Yun, J. L., & Clemens, D. P. 1990, *ApJ*, 365, L73  
 ———. 1994, *AJ*, 108, 612